

## A complete RTM workflow for imaging and model building in the azimuth-angle domain

Nizar Chemingui (PGS)\*, Alejandro Valenciano (PGS), Sergey Frolov (PGS) and Sverre Brandsberg-Dahl (PGS)

Copyright 2017, SBGf - Sociedade Brasileira de Geofísica

This paper was prepared for presentation during the 15<sup>th</sup> International Congress of the Brazilian Geophysical Society held in Rio de Janeiro, Brazil, 31 July to 3 August, 2017.

Contents of this paper were reviewed by the Technical Committee of the 15<sup>th</sup> International Congress of the Brazilian Geophysical Society and do not necessarily represent any position of the SBGf, its officers or members. Electronic reproduction or storage of any part of this paper for commercial purposes without the written consent of the Brazilian Geophysical Society is prohibited.

### Abstract

Robust migration engines and good velocity models are required for optimal imaging of complex and subsalt structures. Ideally, image gathers from the same migration algorithm are also used for the velocity model updating. For that, Reverse Time Migration (RTM) has been established as the tool of choice for imaging complex geologic structures and potential reservoirs.

We discuss here an RTM-based imaging and model-building workflow where the migration image can be mapped into azimuth-angle gathers by direct binning at each time step, whereas the RTM backscattered noise is minimized during the propagation process by the application of an inverse scattering imaging condition (ISIC). Another benefit from the angle decomposition is the application of specular filtering for effective noise suppression in areas where migration artifacts do not conform to the structural interpretation.

We demonstrate the application of the RTM workflow to 3D angle tomographic model building and imaging of full azimuth data. The access to angle gathers at each image location allows the use of optimized post-migration image enhancement strategies for noise suppression and residual corrections to obtain much improved images in both extra-salt and complex sub-salt regions.

### Introduction

Imaging and velocity estimation methods require adequate treatment of subsurface dip, azimuth, and illumination angle to take full advantage of the angular and azimuthal coverage from modern seismic surveys. In this paper we focus on an RTM imaging method that decomposes the pre-stack image into angle and azimuth gathers, which allows for subsequent image post-processing and the application of 3D angle tomography for model building.

There are number of approaches to the generation of RTM angle gathers (e.g. Xu et al., 2011). Here we present an RTM decomposition method based on dynamic binning of the image into angle and azimuth gathers (Crawley et al., 2012; Whitmore et al., 2014). The binning process estimates the incidence angle and azimuth of a reflector from the source and receiver wavefield direction vectors. It also enables specular filtering of the gathers in areas where the noise does not conform to the structural interpretation.

The algorithm uses the pseudo-analytic method that provides accurate, non-dispersive, and nearly artifact-free images (Crawley et al., 2010). It also compensates for

attenuation (Ramos-Martínez et al., 2015) and can handle up to Tilted orthorhombic earth model representations.

Another important feature of the algorithm is the use of an inverse scattering imaging condition (ISIC) to reduce the backscattered noise in the RTM images (Op't Root et al., 2012; Whitmore and Crawley, 2012). ISIC is essential in providing high quality angle gathers free of low wavenumber artifacts.

### RTM Azimuth–Angle Gather Decomposition

RTM is a two-way wave-equation migration method where each shot is imaged onto the subsurface independently. During the imaging process, one can estimate an opening angle and azimuth of a reflector at every image location given the source and receiver wavefield direction vectors:

$$\theta(p_s, p_r) \cong \frac{1}{2} \cos^{-1} \left( \frac{p_s \cdot p_r}{|p_s| |p_r|} \right) \quad (1)$$

where  $p_s$  and  $p_r$  are the direction vectors computed directly from the wavefields,  $S$  and  $R$ :

$$p_s \cong \frac{\nabla S(\bar{x}, t)}{\frac{\partial S(\bar{x}, t)}{\partial t}} \quad p_r \cong \frac{\nabla R(\bar{x}, t)}{\frac{\partial R(\bar{x}, t)}{\partial t}} \quad (2)$$

Figure 1 shows an example of an RTM common image gather sectorized into six azimuths and 46 angle bins from the migration of a full-azimuth survey.

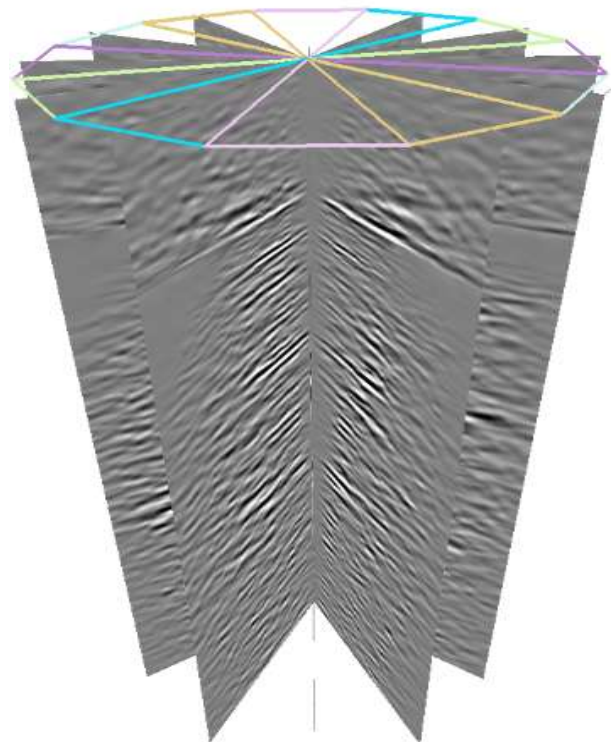


Figure 1. Azimuth-angle gather decomposition of a migrated image from a FAZ survey.

### Inverse Scattering Imaging Condition (ISIC)

The angular decomposition of the RTM image requires removal of the backscattered RTM noise at each time step. To mitigate this problem, we employ an advanced imaging condition that we refer to as inverse scattering imaging condition (ISIC). The definition of ISIC, at a fixed time  $t$ , is given by:

$$I(x, t) = W_1(x, t) \nabla \psi_s(x, t) \cdot \nabla \psi_r(x, T - t) + W_2(x, t) \frac{1}{v^2(x)} \frac{\partial \psi_s(x, t)}{\partial t} \frac{\partial \psi_r(x, T - t)}{\partial t} \quad (3)$$

where  $\Psi_S$  and  $\Psi_R$  are the source and receiver wavefields.

This imaging condition uses two kernels that are combined using appropriate weights to attenuate the backscattered RTM noise (Figure 2). A noise-free image can then be decomposed into volumes corresponding to different subsurface angles and azimuths at every image point  $I(x_s, x_r, \theta, \alpha, t)$  (Figure 3). This enables post-migration processing and estimation of residual curvatures for 3D angle tomography.

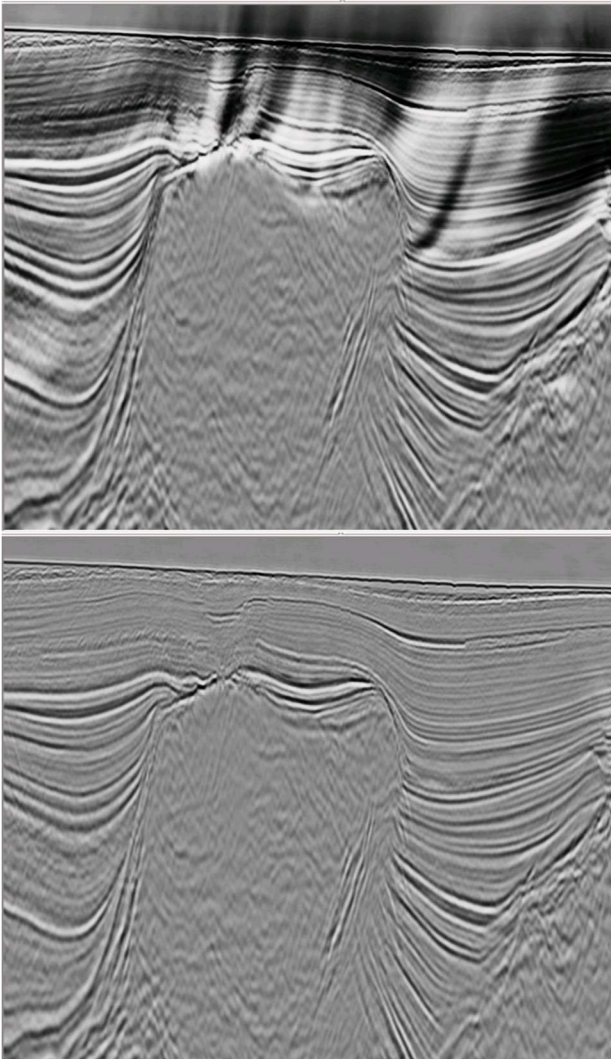


Figure 2. Full RTM stack. Top panel - cross-correlation imaging condition, bottom panel - Inverse Scattering Imaging Condition (ISIC)

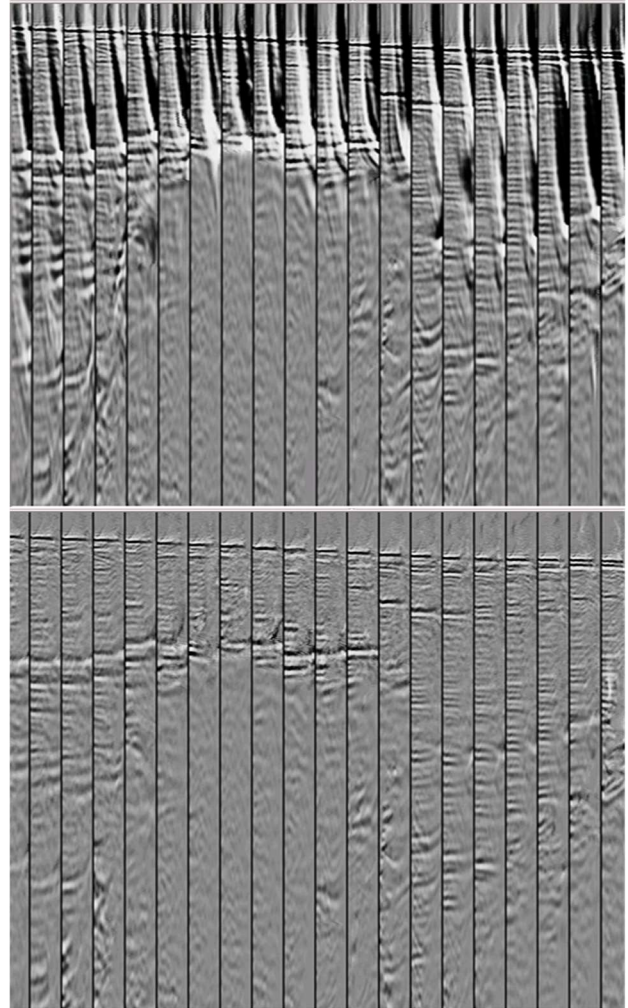


Figure 3. RTM angle gathers. Top panel - cross-correlation imaging condition, bottom panel - Inverse Scattering Imaging Condition (ISIC)

### Specular filtering of angle gathers

In addition to decomposing the image into azimuth angle gathers, the direction vectors can be further utilized for specular filtering. The sum of the source and receiver ray parameters provides the vector normal to the dip, i.e. the dip angle and azimuth of the reflector. This computed normal is compared to the one provided by the structural interpretation (dip field). The difference between the two is used to discriminate specular reflections from artifacts (Figure 4).

### Model updating with 3D RTM angle tomography

The azimuth-angle decomposition of the RTM images enables the estimation of residual depth errors that can be projected onto model updates using angle tomography. The process is very efficient and involves upward ray tracing using the subsurface angles and azimuths that define a unique ray for each subsurface location (Figure 5). We applied the 3D angle tomography to a FAZ survey from the Gulf of Mexico. A small subset of angle gathers and the starting and final tomographic models were extracted for display and are shown in Figure 6. The gathers are displayed with their respective velocity models.

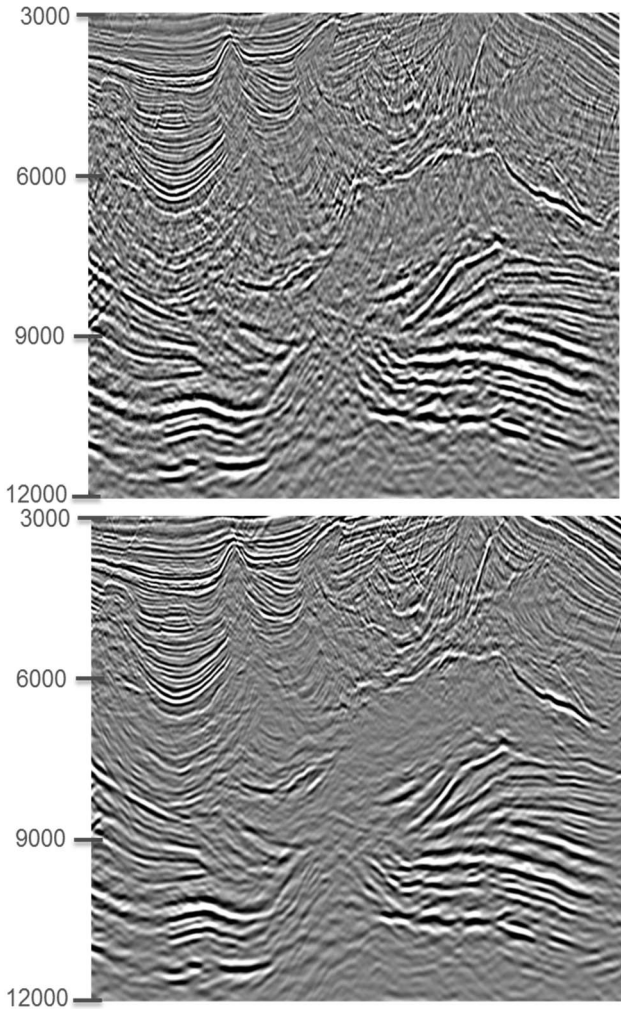


Figure 4. Full stack before (top) and after (bottom) specular filtering.

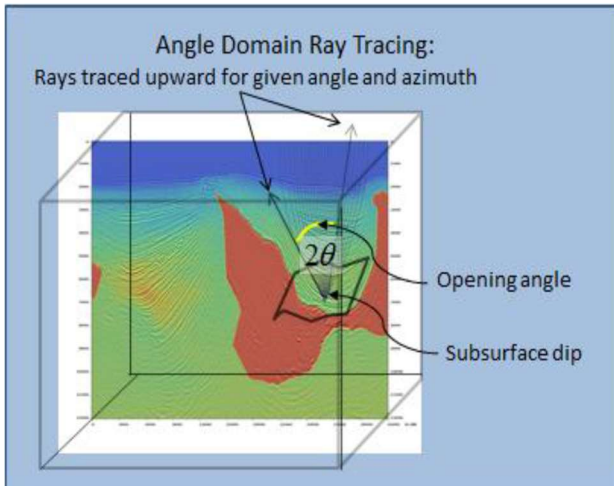


Figure 5. RTM angle domain tomography uses travel times computed by ray tracing upward from reflection points in the subsurface for a set of angles, azimuth and subsurface dip.

**Image enhancement by selective stacking**

Given a final image decomposed into azimuth-angle sectors, we can carefully select parts of it to improve the final stack. The main assumption behind the methodology is that reliable reflections are similarly present in most angle/azimuth volumes.

To measure the similarity between the images, we use the normalized cross-covariance of a pair of images with zero mean,  $I_{iklm}(x)$  and  $I_{jklm}(x)$ :

$$C_{ij}(x) = \frac{\sum_k \sum_l \sum_m \bar{I}_{iklm}(x) \cdot \bar{I}_{jklm}(x)}{\sqrt{\sum_k \sum_l \sum_m \bar{I}_{iklm}(x) \cdot \sum_k \sum_l \sum_m \bar{I}_{jklm}(x)}}$$

where  $x$  is a spatial location  $(x,y,z)$ ,  $i$  and  $j$  are the two volume indices out of the angle-azimuth decomposition,  $k$ ,  $l$  and  $m$  are indices over the inlines, crosslines and  $z$ , respectively.

After forming the covariance matrix, we analyze it to define the optimal set of angles and azimuths that have similar characteristics. Figure 8 shows a segment of a QC volume produced after selective stacking. Parts of the image that were kept for stacking are in red, removed data is not highlighted. The algorithm is able to delineate the extent of the signal. Figure 9 shows the result of selective stacking applied to azimuth-angle sectorized image gathers after post-migration image enhancement. The image has higher signal-to-noise ratio, and the reflectors appear more continuous and coherent. The de-noising effect is more noticeable in the zones where coherent noise with conflicting dip interferes with well-focused reflectors.

**Conclusions**

We show that an RTM-based workflow for imaging and model building in the azimuth-angle domain dramatically improves the imaging of complex structures. The velocity model building by iterative RTM angle tomography is crucial for optimal interpretation of salt bodies and better estimation of subsalt migration velocities. Our 3D angle-gathers are virtually artifact free as we use an inverse scattering imaging condition that effectively removes the backscattering noise during the imaging step. Moreover, the azimuth-angle decomposition enables suppression of migration artifacts by filtering of non-specular events. With access to angle gathers for the whole image volume, we can employ robust image enhancement solutions for muting, editing, noise suppression and residual corrections before stacking of partial images. The selective stacking leads to significantly improved images.

**Acknowledgment**

We thank PGS for permission to publish the results and PGS MultiClient for providing the data.

**References**

Brandsberg-Dahl, S., Chemingui, N., Whitmore D., Crawley, S., Klochikhina, E., and Valenciano, A.A., 2013, 3D RTM angle gathers using an inverse scattering imaging condition. SEG, Expanded Abstracts: pp. 3958-3962.

Crawley, S., Brandsberg-Dahl S., and McClean, J., 2010, 3D TTI RTM using the pseudo-analytic method. SEG Expanded Abstracts: pp. 3216-3220.  
 Frolov, S., Brown, S., Arasanipalai, S., Chemingui, N., 2016, Post-migration image optimization: A Gulf of Mexico case study. SEG, Expanded Abstracts: pp. 4695-4699.  
 Op't Root, T., C. Stolk, and M. V. de Hoop, 2012, Linearized inverse scattering based on seismic reverse-time migration: Journal de Mathématiques Pures et Appliquées, 98, no. 2, 211–238.

Ramos-Martínez, J., Valenciano, A.A., Crawley, S., and Orlovich, M., 2015, Viscoacoustic compensation in RTM using the pseudo-analytical extrapolator. SEG, Expanded Abstracts: pp. 3954-3958.  
 Whitmore, N., and S. Crawley, 2012, Applications of RTM inverse scattering imaging conditions: SEG, Expanded Abstracts.  
 Xu, S., Y. Zhang, and B. Tang, 2011, 3D angle gathers from reverse time migration: Geophysics, 76, no. 2, S77–S92.

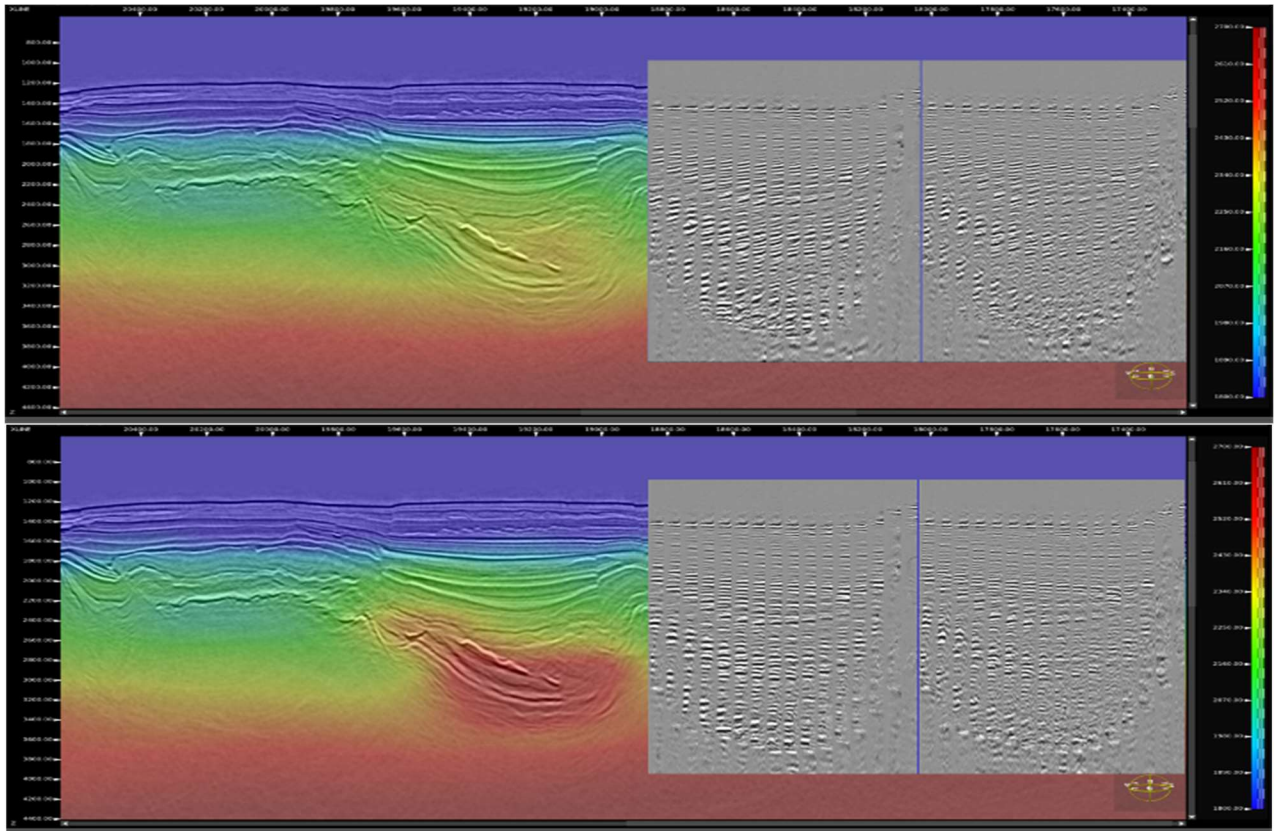


Figure 6. Model, stack and angle gathers for two azimuths. Top – before 3D angle tomography, bottom – after.

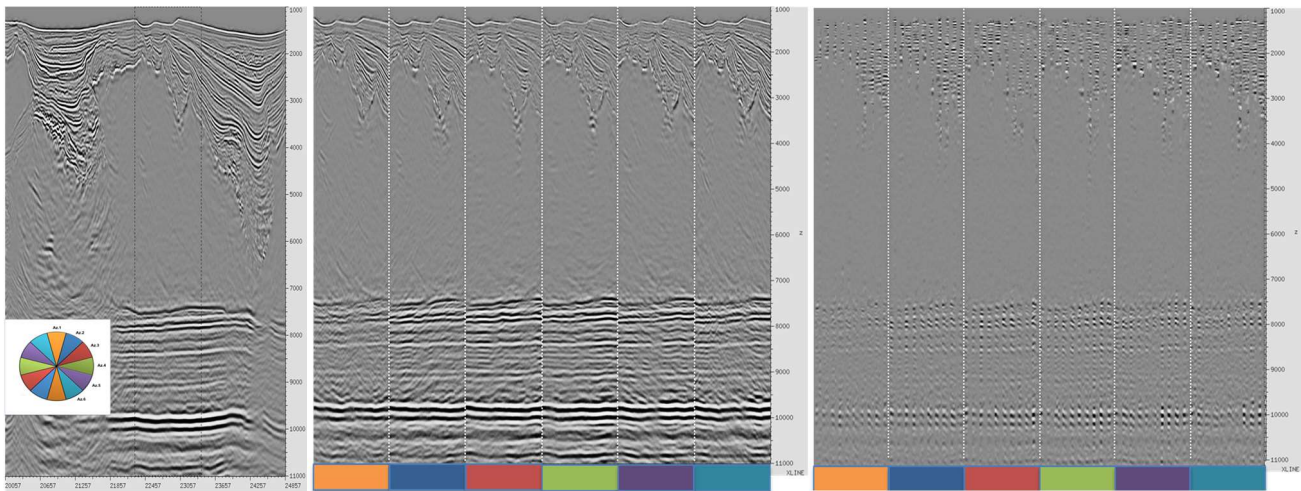


Figure 7. Full stack (left), stacks (center) and angle gathers (right) for each azimuth.

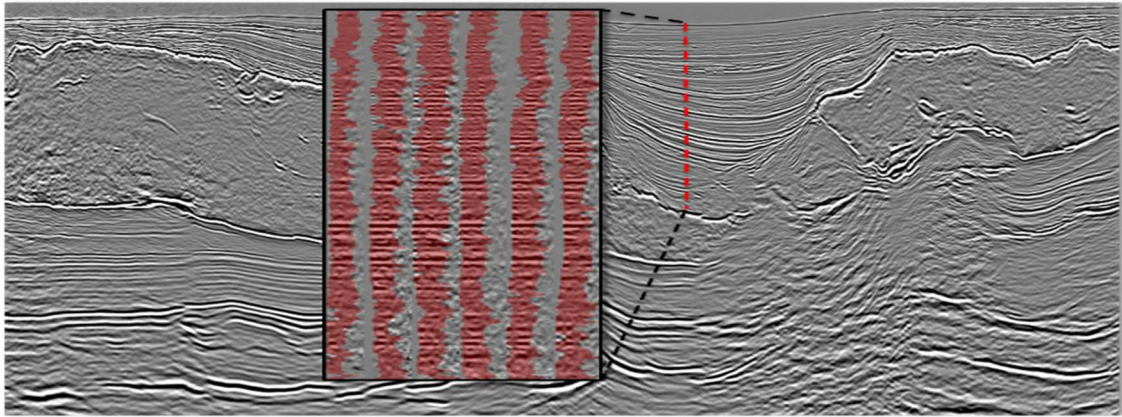


Figure 8. Retained part of azimuth sector angle gather after optimized stacking.

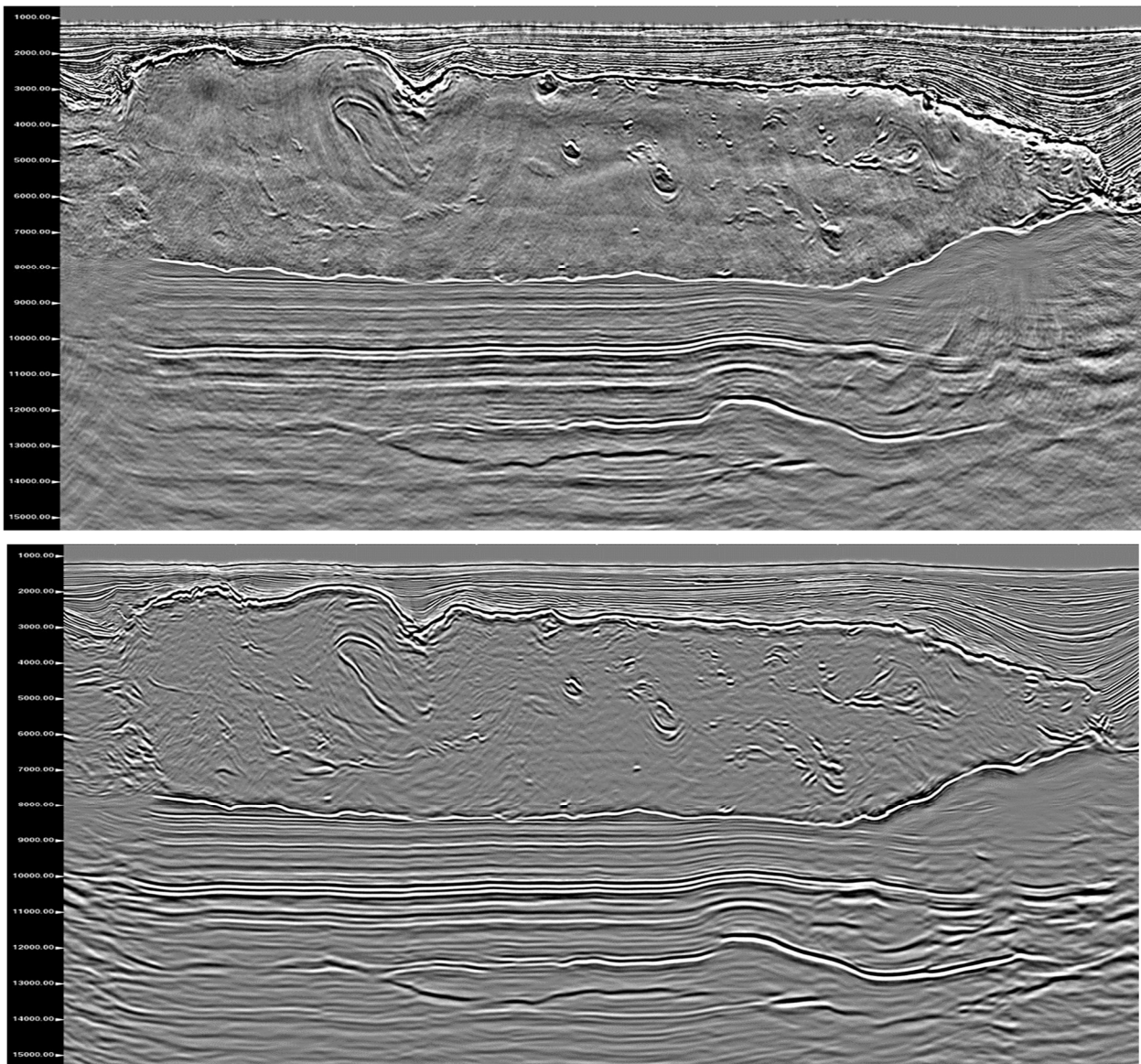


Figure 9. Full stack before (top) and after (bottom) selective stacking.